

Lithium abundance in a sample of solar-like stars

R. López-Valdivia^{1*}, J. B. Hernández-Águila¹, E. Bertone¹, M. Chávez¹,
F. Cruz-Saenz de Miera¹, and E. M. Amazo-Gómez²

¹ *Instituto Nacional de Astrofísica, Óptica y Electrónica, Luis Enrique Erro 1, Tonantzintla, Puebla, 72840, México*

² *Universitäts-Sternwarte München, Scheinerstrasse 1, D-81679 München, Germany*

Accepted 1988 December 15. Received 1988 December 14; in original form 1988 October 11

ABSTRACT

We report on the determination of the lithium abundance $[A(\text{Li})]$ of 52 solar-like stars. For 41 objects the $A(\text{Li})$ here presented corresponds to the first measurement. We have measured the equivalent widths of the 6708 Å lithium feature in high-resolution spectroscopic images ($R \sim 80\,000$), obtained at the Observatorio Astrofísico Guillermo Haro (Sonora, Mexico), as part of the first scientific observations of the revitalized Lunar and Planetary Laboratory (LPL) Echelle Spectrograph, now known as the Cananea High-resolution Spectrograph (CanHiS). Lithium abundances were derived with the Fortran code MOOG, using as fundamental input a set of atmospheric parameters recently obtained by our group.

With the help of an additional small sample with previous $A(\text{Li})$ determinations, we demonstrate that our lithium abundances are in agreement, to within uncertainties, with other works. Two target objects stand out from the rest of the sample. The star BD+47 3218 ($T_{\text{eff}} = 6050 \pm 52$ K, $A(\text{Li}) = 1.86 \pm 0.07$ dex) lies inside the so-called *lithium desert* in the the $A(\text{Li})$ – T_{eff} plane. The other object, BD+28 4515, has an $A(\text{Li}) = 3.05 \pm 0.07$ dex, which is the highest of our sample and compatible with the expected abundances of relatively young stars.

Key words: stars: solar-type; stars: abundances; techniques: spectroscopic.

1 INTRODUCTION

In convective stars, the photospheric lithium abundance $A(\text{Li})$ ¹ decreases with time, because vertical motions transport Li atoms to deeper layers hot enough ($\approx 2.5 \times 10^6$ K) to burn it by proton capture.

The Sun has a very low photospheric $A(\text{Li})$ compared to nearby solar analogs (e. g., Lambert & Reddy 2004), and it is more than 2 dex lower than the meteoric abundance ($A(\text{Li})_{\odot} = 1.05 \pm 0.10$ vs. $A(\text{Li})_{\text{met}} = 3.26 \pm 0.05$; Asplund et al. (2009)). This difference cannot be explained by standard models (e. g., D’Antona & Mazzitelli 1994), consequently, several processes have been proposed: for instance, mass loss (Swenson & Faulkner 1992), angular momentum loss and rotation (Schatzman & Baglin 1991; Pinsonneault et al. 1992; Deliyannis & Pinsonneault 1997; Eggenberger, Maeder & Meynet 2010), magnetic fields (Eggenberger, Maeder & Meynet 2010; Li et al. 2014) or gravity waves (García López & Spruit 1991; Montalbán & Schatzman 2000; Charbonnel & Talon 2005),

all of which induce an extra mixing.

More recently, it has also been suggested that the presence of planets could affect the evolution of Li abundance. Bouvier (2008) and Eggenberger et al. (2012) proposed that a long lasting star-disk interaction during the pre-main-sequence stage could slow down the rotation of the host star, enhancing the rotational mixing and thus destroying more lithium. Théado & Vauclair (2012) investigated the effects of disk matter accretion, that induce diffusive instabilities resulting in an extra mixing episode. Castro et al. (2009) pointed out that a transfer of angular momentum due to planetary migration could increase the mixing efficiency and Li depletion. Additionally, Takeda et al. (2010) confirmed that Li depletion in solar-like stars is more efficient when stellar rotation decelerates.

Even though some authors (e. g., Israelian et al. 2004; Gonzalez 2008; Israelian et al. 2009; Gonzalez 2014; Delgado Mena et al. 2014; Figueira et al. 2014; Gonzalez 2015) claimed to have found that stars with exoplanets show an excess of Li depletion, the existence of a possible $A(\text{Li})$ -planet correlation is still matter of debate, as different works (Ryan 2000; Luck & Heiter 2006; Ghezzi et al. 2010; Baumann et al. 2010; Ramírez et al. 2012) had not found such correlation. Increasing the number of main-sequence

* E-mail: valdivia@inaoep.mx

¹ $A(\text{Li}) = \log(n(\text{Li})/n(\text{H})) + 12$, where n is the number density of atoms.

(MS) stars with known Li abundance is therefore helpful to reach more robust statistical results.

In this work, we present the determination of lithium abundances, measured from the 6708 Å resonance line, for 52 solar-like stars of intermediate brightness. For 41 of the targets our analysis represents the first Li measurement. The working sample and observations are described in Section 2. In Section 3, we detail the procedure followed for deriving abundances and, in Section 4, we discuss the results.

2 SAMPLE DEFINITION AND OBSERVATIONS

The stellar sample is somewhat inhomogeneous, but reflects a continuation of a global project aimed at determining stellar parameters (T_{eff} / $\log g$ / $[M/H]$) as well as abundances of individual chemical species of a sample of Sun-like stars (types G0-G3) on the MS. As an initial step, we have selected 30 stars from our previous work (López-Valdivia et al. 2014), 12 objects of which correspond to metal-rich stars (SMR; $[M/H] \geq 0.16$ dex). This latter sub-sample is in fact composed by all the SMR stars that are sufficiently bright to allow high resolution observations with the instrument briefly described below. The sample is complemented with 11 stars, that accomplish the criteria in spectral type and luminosity class of López-Valdivia et al. (2014), included in the catalog of Casagrande et al. (2011) for which no previous Li determination has been reported. For comparison purposes, we also observed 11 stars from the work of Ramírez et al. (2012) who provide their Li abundances.

The full sample is listed in Table 1, where we give some basic data and the results of our analysis. Columns 1-13 provide the star identification, the spectral type, the leading atmospheric parameters and their uncertainties (from López-Valdivia et al. 2014; Casagrande et al. 2011), the 6708 Å Li line equivalent width (EW) and its uncertainty, as described in the following section, and the last column gives a label for the source of stellar parameters.

The spectroscopic data were collected at the 2.1 meter telescope of the Observatorio Astrofísico Guillermo Haro, located in Mexico, using the Cananea High-resolution Spectrograph (CanHiS), as part of the first scientific observations of this instrument², at this facility. CanHiS is equipped with filters, that provide access to ~ 40 Å-wide wavelength intervals in single diffraction orders. Our observations were centered at 6710 Å, with a spectral resolving power of $R \sim 80000$ and a typical signal-to-noise ratio (S/N) of about 100. All the data collected (at least 3 images for each star) were reduced with IRAF, following standard procedures: bias subtraction, flat-field correction, cosmic-ray removal, wavelength calibration through an internal UNe lamp and, finally, continuum normalization. We then transformed all the spectra to the rest frame, using the spectrum of the Sun by Kurucz et al. (1984) as template. For each star we co-added its spectra weighted by their S/N. In Fig. 1 we present the

spectra of the Li region of the 52 solar-like stars observed in this work.

3 ABUNDANCES DETERMINATION

In this Section we will present the procedure that we carried out for measuring the Li abundance of the stellar sample.

3.1 Photospheric parameters and model atmospheres

We collected the T_{eff} , the surface gravity ($\log g$), the global metallicity ($[M/H]$) and their uncertainties (see Table 1, column 4 to 9) from two works. The first one is López-Valdivia et al. (2014), where T_{eff} , $\log g$ and $[M/H]$ were simultaneously determined using a set of Lick-like indices and intermediate-resolution spectroscopic observations. The second work is Casagrande et al. (2011), where the T_{eff} is obtained through the infrared flux method (Blackwell & Shallis 1977; Casagrande et al. 2006), the $\log g$ from the fundamental relation, which involves bolometric luminosity and T_{eff} and finally the metallicity as $[Fe/H]$ from a calibration of Strömgren colours³. The last column of Table 1 reports the source of the stellar parameters for each star of our sample.

By means of the 22 object in common in the López-Valdivia et al. (2014) and Casagrande et al. (2011) samples, we investigated possible systematic differences in the T_{eff} scales, which is the most important parameter for Li abundance determination (see Sect. 3.3.1). The data, plotted in Fig. 2, indeed show a tendency of Casagrande et al. (2011) temperatures to be slightly higher, mostly at the cooler end. Since López-Valdivia et al. (2014) T_{eff} scale was constructed to optimize the parameters of G0-G3 MS stars and considering that Casagrande et al. (2011) stated that their T_{eff} are on average 100 K hotter than previous analyses, we transformed the Casagrande et al. (2011) temperatures to the López-Valdivia et al. (2014) scale through a linear regression of data displayed in Fig. 2:

$$T_{\text{eff,cor}} = \frac{T_{\text{eff,Cas}} - 1247.86}{0.80} \quad (1)$$

where $T_{\text{eff,Cas}}$ is the temperature reported in Casagrande et al. (2011) and $T_{\text{eff,cor}}$ is the corrected one.

We then determined a model atmosphere for each star by interpolating the Castelli & Kurucz (2003) grid of models in the T_{eff} , $\log g$ and $[M/H]$ 3-dimensional space. For all cases, we used the microturbulence velocity $\xi = 2 \text{ km s}^{-1}$ (see also Section 3.3.1).

3.2 Equivalent widths

We measured the EW of the 6708 Å lithium line with a flux fitting procedure. We simultaneously fit the Li and the adjacent Fe I line at 6707.44 Å using three Gaussian functions: two of them are necessary to reproduce the two-component (simply called Li₁ and Li₂) asymmetric Li line,

² CanHiS was donated in 2009 by the University of Arizona to our institute; it was originally known as LPL Echelle Spectrograph and used at the 61-inch Catalina Telescope to carry out observations of Solar System bodies at specific spectral regions (for more details about its original design see Hunten et al. 1991).

³ We used the overall metallicity reported in the electronic version of the catalog of Casagrande et al. (2011), instead of $[Fe/H]$.

Table 1. Physical parameters and Li abundance of the stellar sample. Temperatures from Casagrande et al. (2011) were corrected following Eq. 1.

Object	V	SType	T_{eff} (K)	σ (K)	$\log g$ (dex)	σ (dex)	[M/H] (dex)	σ (dex)	EW(Li) (mÅ)	σ EW(Li) (mÅ)	A(Li) (dex)	σ A(Li) (dex)	S
HD 5649	8.70	G0V	5830	52	4.45	0.22	-0.08	0.04	27.5	3.6	2.05	0.08	L
BD+60 402	10.26	G0V	5985	72	4.30	0.40	0.22	0.09	58.0	9.5	2.58	0.12	L
HD 13403	7.00	G3V	5565	204	4.74	-	-0.29	-	< 5.5	-	< 1.04	-	C
HD 16894	8.02	G2V	5500	70	4.05	0.30	-0.10	0.09	6.4	1.0	1.1	0.09	L
BD+60 600	8.65	G0V	5655	47	3.95	0.20	0.20	0.07	78.0	1.2	2.51	0.04	L
HD 232824	9.52	G2V	5900	67	4.15	0.35	0.16	0.08	61.7	5.7	2.56	0.08	L
HD 237200	9.66	G0V	6045	55	4.25	0.32	0.18	0.05	18.3	3.1	2.03	0.09	L
HD 26710	7.18	G2V	5815	47	4.55	0.20	-0.04	0.04	60.8	7.1	2.47	0.08	L
HD 31867	8.05	G2V	5590	57	4.40	0.25	-0.10	0.06	< 4.9	-	< 1.03	0.08	L
HD 33866	7.87	G2V	5481	123	4.33	-	-0.07	-	11.0	1.6	1.28	0.13	C
HD 41708	8.03	G0V	5998	58	4.55	-	0.08	-	38.1	1.2	2.36	0.05	C
HD 42807 ^a	6.44	G2V	5617	80	4.53	-	-0.11	-	43.8	5.5	2.10	0.10	C
HD 77730	7.39	G2V	5698	80	4.13	-	-0.05	-	18.9	2.8	1.75	0.10	C
HD 110882	8.87	G1V	5880	50	4.40	0.25	-0.28	0.04	38.8	0.8	2.26	0.05	L
HD 110884	9.11	G3V	5905	87	4.30	0.40	-0.26	0.08	< 3.9	-	< 1.20	-	L
HD 111513 ^a	7.35	G1V	5723	80	4.31	-	0.12	-	11.4	1.7	1.53	0.10	C
HD 111540	9.54	G1V	5840	47	4.20	0.25	0.14	0.05	23.1	5.2	1.97	0.12	L
HD 124019	8.56	G2V	5685	57	4.65	0.25	-0.18	0.06	19.0	2.6	1.73	0.08	L
HD 126991	7.90	G2V	5360	107	3.15	0.40	-0.34	0.14	< 4.7	-	< 0.79	-	L
HD 127913	9.14	G2V	5475	65	4.45	0.20	-0.12	0.08	17.5	1.2	1.50	0.07	L
HD 129357	7.83	G2V	5775	52	4.30	0.22	-0.14	0.05	< 4.4	-	< 1.14	-	L
HD 130948 ^a	5.88	F9IV-V	5885	80	4.42	-	-0.09	-	93.8	10.0	2.84	0.12	C
HD 135145 ^a	8.35	G0V	5997	80	4.14	-	-0.02	-	20.3	2.8	2.04	0.10	C
HD 135633	8.46	G0V	6095	67	4.25	0.40	0.22	0.06	69.0	0.9	2.79	0.06	L
HD 140385 ^a	8.57	G2V	5735	60	4.60	0.27	-0.16	0.08	< 5.6	-	< 1.21	-	L
HD 145404	8.54	G0V	5920	82	4.43	-	-0.16	-	37.2	4.6	2.28	0.10	C
HD 152264	7.74	G0V	6177	73	4.09	-	0.02	-	53.6	6.9	2.70	0.10	C
BD+29 2963	8.42	G0V	5865	55	4.70	0.22	0.00	0.04	< 5.9	-	< 1.36	-	L
HD 156968 ^a	7.97	G0V	6105	96	4.42	-	-0.03	-	18.9	1.4	2.09	0.09	C
HD 168874 ^a	7.01	G2IV	5696	80	4.41	-	-0.05	-	65.4	9.6	2.41	0.12	C
BD+28 3198	8.66	G2V	5840	35	4.00	0.17	0.24	0.05	59.1	8.1	2.49	0.09	L
HD 182407	7.77	G0V	5953	70	3.94	-	0.25	-	< 3.6	-	< 1.22	-	C
TYC 2655-3677-1	9.93	G0V	6220	47	4.15	0.27	0.28	0.05	38.9	6.2	2.54	0.10	L
HD 187237 ^a	6.88	G2IV-V	5687	62	4.42	-	-0.04	-	89.2	9.8	2.63	0.10	C
HD 187548	7.98	G0V	6170	42	4.80	0.17	-0.24	0.03	49.3	2.4	2.63	0.05	L
HD 333565	8.75	G1V	5990	52	4.45	0.27	0.12	0.05	44.2	6.5	2.43	0.09	L
HD 228356	9.07	G0V	6055	37	4.00	0.20	0.16	0.05	63.4	5.6	2.71	0.07	L
HD 193664 ^a	5.93	G3V	5942	112	4.47	-	-0.11	-	30.2	2.6	2.19	0.11	C
BD+47 3218	8.70	G0V	6050	52	4.05	0.30	0.16	0.06	12.6	1.30	1.86	0.07	L
HD 199960 ^a	6.21	G1V	5895	80	4.24	-	0.22	-	61.0	8.1	2.54	0.11	C
HD 201860	8.65	G0V	5620	107	3.66	-	-0.02	-	30.9	0.3	1.93	0.10	C
HD 210460	6.19	G0V	5357	80	3.58	-	-0.17	-	< 4.8	-	< 0.80	-	C
HD 210483 ^a	7.59	G1V	5878	95	4.19	-	-0.01	-	19.8	2.7	1.93	0.11	C
TYC 3973-1584-1	10.74	G2V	6000	45	4.45	0.22	0.20	0.05	47.2	6.4	2.48	0.09	L
TYC 3986-3381-1	10.37	G2V	5855	57	4.15	0.25	0.26	0.07	79.1	5.1	2.68	0.07	L
HD 239928	8.69	G2V	5870	67	4.40	0.30	0.06	0.06	17.3	2.4	1.86	0.09	L
HD 212809	8.64	G2V	5975	55	4.55	0.27	0.16	0.05	33.5	2.6	2.27	0.06	L
HD 217924	7.22	G0V	5900	52	4.85	0.20	-0.10	0.05	17.2	3.6	1.87	0.11	L
BD+28 4515	8.73	G2V	5580	40	3.50	0.17	-0.22	0.06	146.0	6.8	3.05	0.07	L
HD 218633	8.19	G2V	5385	70	3.50	0.30	-0.32	0.10	< 6.4	-	< 0.96	-	L
HD 218730	7.32	G0V	5922	83	4.45	-	0.09	-	54.8	9.5	2.50	0.12	C
HD 220334	6.62	G2V	5801	91	4.13	-	0.14	-	87.9	3.0	2.72	0.09	C

^a Star with previous determination of A(Li).

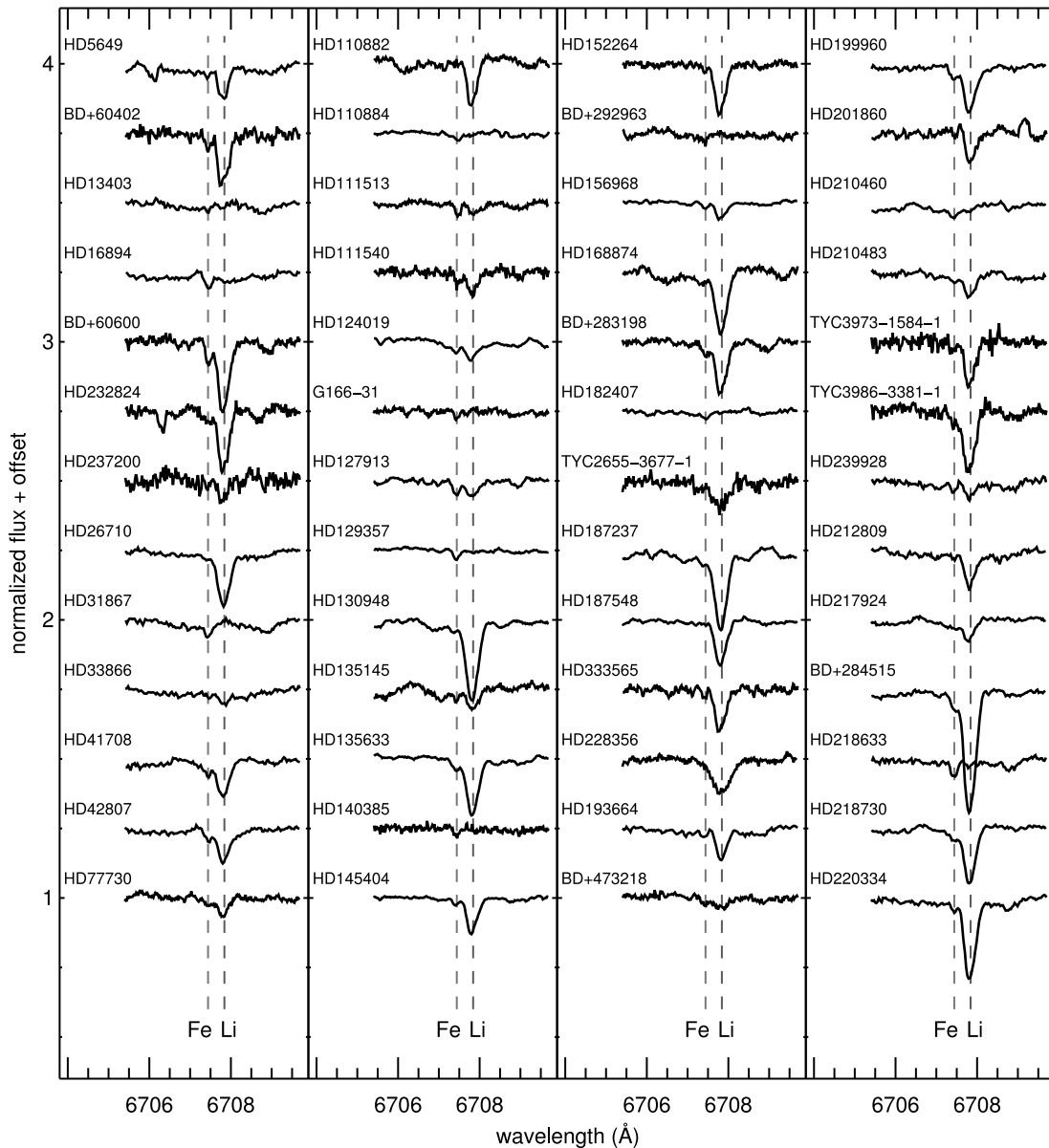


Figure 1. Normalized spectra of our stellar sample, centered around the Li line. The position of the Li line and of the adjacent Fe line is indicated by vertical dashed lines.

while the third is needed to quantify the Fe contamination. The parameters of the Gaussian functions (central wavelength, width and amplitude) were modified within appropriate values for each star to obtain the best fit, which was also validated through visual inspection. The integral of the sum of the Li_1 and Li_2 Gaussians provides the $\text{EW}(\text{Li})$.

We adopted a Monte Carlo procedure to estimate the error in the measurement of $\text{EW}(\text{Li})$. For each star, we determined the standard deviation of the flux in two wavelength regions, 6705.4–6707.0 Å and 6708.6–6709.7 Å, bracketing the Li line. We used this value as the width of a Gaussian distribution which provides the random noise value that we added to the observed spectrum and we repeated the fitting procedure previously described. We carried out 1000 realizations to obtain the EW distributions of the three Gaussian functions, whose standard deviations we added in quadrature

to obtain the error $\sigma_{\text{EW}(\text{Li})}$. The $\text{EW}(\text{Li})$ values, along with their errors, are reported in columns 10 and 11 of Table 1.

3.3 Lithium abundances computation

To carry out the determination of the Li abundances, we made use of the driver *abfind* of the February 2013 version of the Fortran code MOOG (Snedden 1973), which performs an adjustment of the abundances to match a single-line equivalent width. This code requires a model atmosphere and the physical parameters of a list of absorption lines to compute atomic abundances. We assumed the Li line to be a single electronic transition centered at $\lambda 6707.84$ Å with $\log gf = +0.167$, that corresponds to the average wavelength and the sum of the gf values of the two compo-

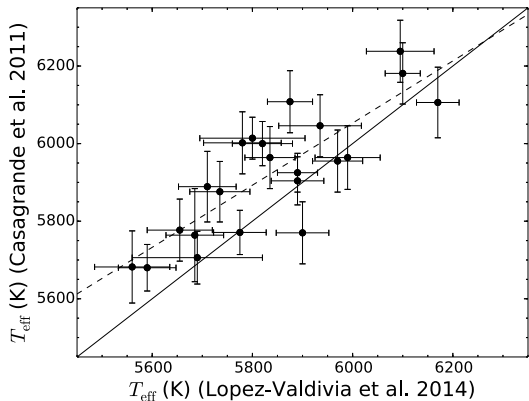


Figure 2. Comparison of T_{eff} from López-Valdivia et al. (2014) and Casagrande et al. (2011) for 22 solar-like stars in common. The dashed line shows the best linear regression, while the solid line indicates the one-to-one relation.

nents (Li_1 : $\lambda=6707.76 \text{ \AA}$, $\log gf=-0.009$; Li_2 : $\lambda=6707.91 \text{ \AA}$, $\log gf=-0.309$), obtained from the Vienna Atomic Line Database (VALD; Kupka et al. 1999).

3.3.1 Error of Li abundances

The main sources of error in the determination of the Li abundance are related with uncertainties on the stellar parameters and on the EW measurement. In order to have an estimation of the errors introduced by the atmospheric parameters, we conducted some theoretical tests. We varied, one at a time, the four main stellar parameters (T_{eff} , $\log g$, $[\text{M}/\text{H}]$ and ξ), maintaining the other three fixed, and compute the Li abundance, assuming an $\text{EW}(\text{Li}) = 50 \text{ m\AA}$, to measure the variations in $\text{A}(\text{Li})$. The chosen fixed values were 5750 K, 4.5 dex, 0.0 dex, and 2.0 km s^{-1} , for T_{eff} , $\log g$, $[\text{M}/\text{H}]$ and ξ , respectively. We obtained the following results: a change in effective temperature of $\Delta T_{\text{eff}} = 100 \text{ K}$ produces a lithium abundance variation of $\Delta \text{A}(\text{Li}) = 0.09 \text{ dex}$, while a very small change in abundance of $\Delta \text{A}(\text{Li}) = 0.01 \text{ dex}$ is obtained if we modify the other parameters by $\Delta \log g = 0.5 \text{ dex}$, $\Delta [\text{M}/\text{H}] = 0.15 \text{ dex}$ and $\Delta \xi = 1 \text{ km s}^{-1}$. These results, very similar to those from previous works (e. g., Chen et al. 2001; Charbonnel & Primas 2005), indicate that the uncertainty in the T_{eff} is by far the dominant source of error. Furthermore, our assumption of a single value for ξ of our models does not introduce a significant systematic error in the Li abundance. This choice is also supported, for instance, by the work of Gray, Graham & Hoyt (2001), who derived a ξ between 1 and 2 km s^{-1} for their sample of F7–G2 MS stars.

We calculated the contribution of the EW uncertainty to the error on the Li abundance $[\sigma \text{A}(\text{Li})]$ by computing the $\text{A}(\text{Li})$ for the values $\text{EW}(\text{Li}) \pm \sigma \text{EW}(\text{Li})$ and dividing their difference by half. The total $\sigma \text{A}(\text{Li})$ is the sum in quadrature of the errors on T_{eff} and EW. All results are reported in Table 1.

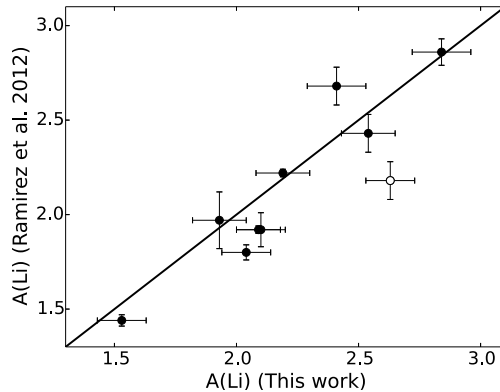


Figure 3. Comparison of the lithium abundance of the stars in common with Ramírez et al. (2012). HD 187237 (see discussion in text) is represented by an empty square, while the solid line indicates the one-to-one relation.

4 DISCUSSION

In order to put the Li abundance of our sample in the context of the known results for solar-like stars, we used the work of Ramírez et al. (2012) as a reference, as it is, to date, the largest homogeneous compilation of lithium abundance of MS and subgiants stars. They derived stellar parameters and Li abundances for 671 stars and included measurements from the literature to construct a catalog of 1381 FGK dwarf and subgiant stars. Analyzing the distribution of data in the $\text{A}(\text{Li})-T_{\text{eff}}$ plane, they confirmed that, in the interval $5950 \leq T_{\text{eff}} \leq 6100 \text{ K}$, stars appear to be neatly separated into two groups of high and low Li abundance, creating an avoidance region, called *lithium desert*, as was suggested for the first time by Chen et al. (2001). These authors proposed that the low-Li side of the $\text{A}(\text{Li})-T_{\text{eff}}$ diagram is populated by evolved lithium dip objects (Boesgaard & Tripicco 1986), that might burn the Li during the pre-MS stage. However, Ramírez et al. (2012) argues against this suggestion, based on their analysis of the mass-metallicity correlation (see also Balachandran 1995; Cummings et al. 2012) of their whole sample, which includes the Chen et al. (2001) data. They also show that there are no young stars (age < 2 Gyr) at the lower side of the *lithium desert*, suggesting that the mechanism that depletes surface lithium in the objects that populate that region should take place during the MS or subgiant phases. However, Ramírez et al. (2012) do not further speculate on the nature of this mechanism.

In total, we have 11 stars in common with Ramírez et al. (2012); however, for the star HD 140385 we have only upper limits and was excluded from the comparison. In Fig. 3, we present the comparison for the remaining common 10 stars, whose $\text{A}(\text{Li})$ are reported in Table 2. The star HD 187237 presents the largest discrepancy of 0.45 dex. In order to achieve the same lithium abundance reported in Ramírez et al. (2012), this object should have half the EW measured in our work, which would represent a 4.5σ anomaly. Since, the EW measurement for this star is one of our best determinations, and the stellar parameters used in both works are not so different, we do not have a clear cause for the discrepancy. In the following analysis, we exclude this star too. In general, we found a good agreement between

Table 2. The lithium abundances and stellar parameters of the stars in common with Ramírez et al. (2012).

Object	A(Li)	σ A(Li)	T_{eff}	$\log g$	[Fe/H]	A(Li)	σ A(Li)
	Our	Our	Ramírez	Ramírez	Ramírez	Ramírez	Ramírez
HD 42807	2.10	0.10	5674	4.51	-0.04	1.92	0.09
HD 111513	1.53	0.10	5811	4.32	0.11	1.44	0.03
HD 130948	2.84	0.12	5942	4.39	-0.11	2.86	0.07
HD 135145	2.04	0.10	5858	4.09	-0.08	1.80	0.04
HD 156968	2.09	0.09	5901	4.36	-0.14	1.92	0.02
HD 168874	2.41	0.12	5858	4.44	0.01	2.68	0.10
HD 187237	2.63	0.10	5792	4.43	0.02	2.18	0.10
HD 193664	2.19	0.11	5902	4.42	-0.14	2.22	0.02
HD 199960	2.54	0.11	5833	4.20	0.13	2.43	0.10
HD 210483	1.93	0.11	5834	4.14	-0.12	1.97	0.15

the A(Li) determined in this work and those determined in Ramírez et al. (2012): on average, we found a difference of +0.05 dex (our minus Ramírez et al. 2012 data). This offset is partly caused by adopting different stellar parameters (mainly different T_{eff}) and/or different atomic data.

Figure 4 presents the A(Li) vs. T_{eff} distribution of our results and their comparison with the complete Ramírez et al. (2012) compilation. It allows us to address three issues.

Super metal-rich stars.

Our stellar sample includes 12 SMR stars of López-Valdivia et al. (2014) ($[M/H]>+0.16$ dex) plus 2 from Casagrande et al. (2011), indicated with red symbols in Fig. 4. It is worthwhile mentioning that SMR stars have become a particularly interesting class, not only because they are important for modeling the chemical evolution of the Galaxy, but also for their positive correlation with the presence of giant planets (e. g., Gonzalez 1998; Santos, Israelian & Mayor 2001; Fischer & Valenti 2005).

The distribution of the Li abundances of our SMR stars is similar to that of the rest of our sample and it also resembles that of the SMR stars in Ramírez et al. (2012). All but three objects lie in the high abundance range of $2.25 < A(\text{Li}) < 2.80$ dex. In the case of the coolest object, BD+60 600, its A(Li)=2.51 dex is quite higher than the median value for its T_{eff} class. On the warmer side, 3 stars show a lower than average Li abundance ($A(\text{Li})<2.10$ dex): HD 237200, BD+47 3218, and HD 182407. The case of BD+47 3218 is discussed below in more detail.

BD+47 3218: the star in the *lithium desert*.

The star BD+47 3218 has $T_{\text{eff}}=6050\pm 52$ K and $A(\text{Li})=1.86\pm 0.07$ dex: these values locate it inside the *lithium desert*, at 1σ in the case of T_{eff} and at 1.7σ in the case of Li abundance. If we consider our possible small over-estimation of the A(Li) with respect to the Ramírez et al. (2012) scale, the star would move further inside the *lithium desert*. Encouraged by this finding, we additionally searched the literature for new A(Li) determinations for MS and subgiants stars from 2012 to date. In total, we found 17 works (Mishenina et al. 2012; Cummings et al. 2012; Li et al. 2012; Monaco et al. 2012; Pace et al. 2012;

Schaeuble & King 2012; Xing et al. 2012; Xing & Xing 2012; Boesgaard et al. 2013; François et al. 2013; Takeda et al. 2013; Gonzalez 2014; Delgado Mena et al. 2014; Önehag et al. 2014; Dobrovolskas et al. 2014; Önehag et al. 2014; Gonzalez 2015), whose results provide 2 more stars within the *lithium desert* boundaries: HD 44985 ($T_{\text{eff}}=6004$ K and $A(\text{Li})=1.87$ dex; Gonzalez 2014) and the star #58440 of M4 ($T_{\text{eff}}=5979$ K and $A(\text{Li})=1.82$ dex; Monaco et al. 2012). Keeping in mind that the A(Li) values come from different works, we can point out two possible conclusions regarding the existence of a *lithium desert*:

- i) If there actually is a short-lived mechanism responsible for the *lithium desert*, as suggested by Ramírez et al. (2012), the stars BD+47 3218, HD 44985 and #58440 in M4 represent a good benchmark to investigate it.
- ii) The *lithium desert* is just a statistical product.

The Li-rich star BD+28 4515.

The star with the highest lithium abundance in our sample is BD+28 4515, with $A(\text{Li})=3.05$ dex. Comparing with the Ramírez et al. (2012) data, this value is the highest in a bin of temperature of 400 K, from 5350 to 5750 K. Within this T_{eff} range there is a total of 228 objects, from the Ramírez et al. (2012) and our samples, emphasizing the peculiarity of BD+28 4515. From our literature revision, we found 3 more stars in the same T_{eff} interval with $A(\text{Li})>3.0$ dex: HD 287927 ($A(\text{Li})=3.24$ dex; Xing et al. 2012), BD+07 582 ($A(\text{Li})=3.26$ dex; Xing et al. 2012), and HD 285840 ($A(\text{Li})=3.02$ dex; Xing & Xing 2012). They are all classified as weak line T Tauri stars (Xing 2010). Using the available data in the literature, we constructed the spectral energy distribution (SED) of BD+28 4515 and compared it, in Fig. 5, with its synthetic SED interpolated in the Castelli & Kurucz (2003) grid, adopting the stellar parameters reported in Table 1. Even though we notice the lack of the distinctive infrared excess of a classical T-Tauri star, the AKARI point, which might reflect an emission of the $10 \mu\text{m}$ silicate feature, appears to be in excess, however at 2σ significance only. We cannot rule out a possible weak line T-Tauri nature for BD+28 4515. Its high lithium abundance is compatible with the values of the Pleiades (see Fig. 2 of Deliyannis et al. 2002), which may be an indication of a relatively young age.

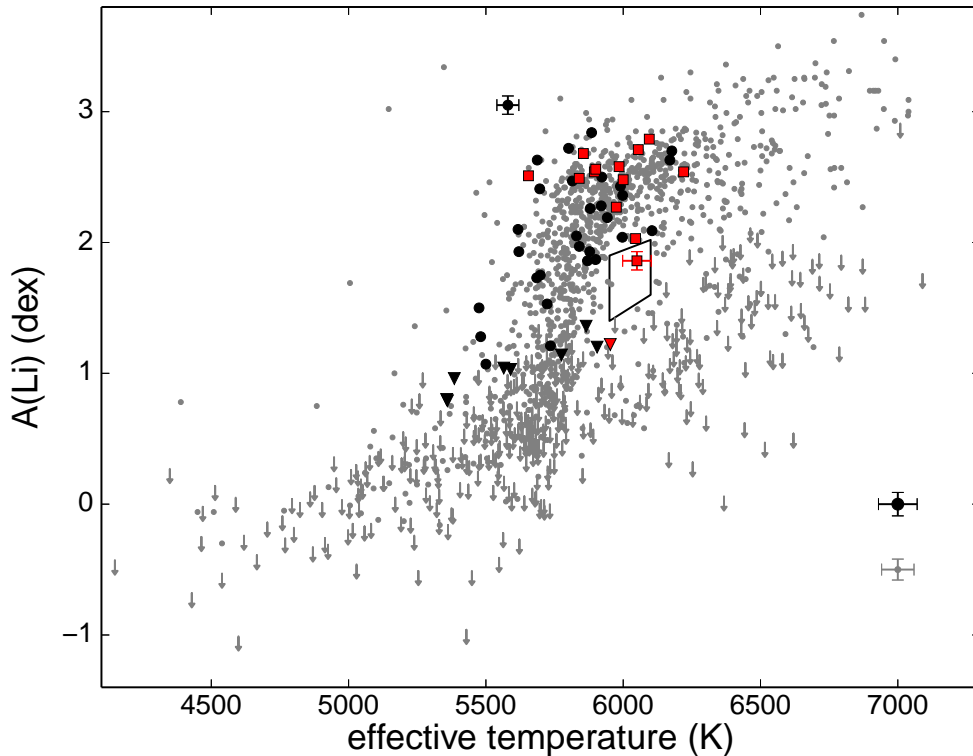


Figure 4. Distribution of lithium abundance with T_{eff} . Black filled circles indicate stars in our sample with $[M/H] < 0.16$ dex, red squares show our SMR stars, and downward triangles mark 3σ upper limits. Grey dots and downward arrows represent Ramírez et al. (2012) determinations and upper limits. The polygon shows the so called *lithium desert*. At the bottom right of the panel, we show the average errors for this work (black) and Ramírez et al. (2012) (gray).

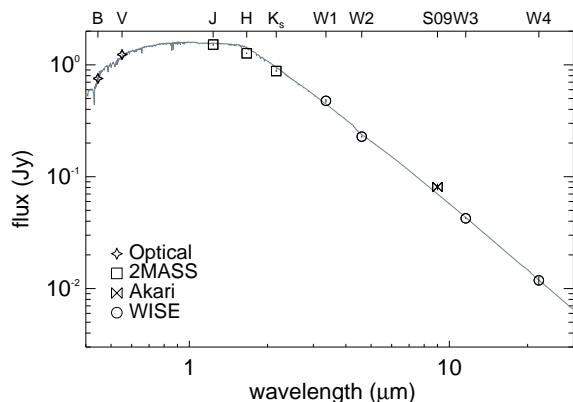


Figure 5. Optical and infrared SED of BD+28 4515. The symbols show the observed photometry, while the solid line represents the synthetic photospheric emission. Error bars are plotted, but they are in most cases much smaller than the symbol size.

ACKNOWLEDGEMENTS

We want to dedicate this paper to the memory of Don Hunten who kindly donated the LPL Echelle Spectrograph to INAOE. We also thank Ann Sprague who gave us a useful tutorial on the use of the spectrograph. RLV, EB and MC would like to thank CONACyT for financial support through

grants SEP-2011-169554 and SEP-2009-134985. This research has made use of the SIMBAD data base, operated at CDS, Strasbourg, France.

REFERENCES

- Asplund, M., Grevesse, N., Sauval, A. J., & Scott, P. 2009, *ARA&A*, 47, 481
- Balachandran, S. 1995, *ApJ*, 446, 203
- Baumann, P., Ramírez, I., Meléndez, J., Asplund, M., & Lind, K. 2010, *A&A*, 519, AA87
- Blackwell, D. E., & Shallis, M. J. 1977, *MNRAS*, 180, 177
- Boesgaard, A. M., & Tripicco, M. J. 1986, *ApJ*, 302, L49
- Boesgaard, A. M., Roper, B. W., & Lum, M. G. 2013, *ApJ*, 775, 58
- Bouvier, J. 2008, *A&A*, 489, L53
- Casagrande, L., Portinari, L., & Flynn, C. 2006, *MNRAS*, 373, 13
- Casagrande, L., Schönrich, R., Asplund, M., et al. 2011, *A&A*, 530, A138
- Castelli, F., & Kurucz, R. L. 2003, *Modelling of Stellar Atmospheres*, IAU Symp., 210, 20P
- Castro, M., Vauclair, S., Richard, O., & Santos, N. C. 2009, *A&A*, 494, 663
- Cayrel de Strobel, G., & Cayrel, R. 1989, *A&A*, 218, L9
- Charbonnel, C., & Primas, F. 2005, *A&A*, 442, 961

- Charbonnel, C., & Talon, S. 2005, *Science*, 309, 2189
- Chen, Y. Q., Nissen, P. E., Benoni, T., & Zhao, G. 2001, *A&A*, 371, 943
- Cummings, J. D., Deliyannis, C. P., Anthony-Twarog, B., Twarog, B., & Maderak, R. M. 2012, *AJ*, 144, 137
- D'Antona, F., & Mazzitelli, I. 1994, *ApJS*, 90, 467
- Delgado Mena, E., Israelian, G., González Hernández, J. I., et al. 2014, *A&A*, 562, AA92
- Delgado Mena, E., Bertrán de Lis, S., Adibekyan, V. Z., et al. 2015, *A&A*, 576, A69
- Deliyannis, C. P., & Pinsonneault, M. H. 1997, *ApJ*, 488, 836
- Deliyannis, C. P., Steinhauer, A., & Jeffries, R. D. 2002, *ApJL*, 577, L39
- Dobrovolskas, V., Kučinskas, A., Bonifacio, P., et al. 2014, *A&A*, 565, AA121
- García López, R. J., & Spruit, H. C. 1991, *ApJ*, 377, 268
- Eggenberger, P., Haemmerlé, L., Meynet, G., & Maeder, A. 2012, *A&A*, 539, A70
- Eggenberger, P., Maeder, A., & Meynet, G. 2010, *A&A*, 519, L2
- Figueira, P., Faria, J. P., Delgado-Mena, E., et al. 2014, *A&A*, 570, AA21
- Fischer, D. A., & Valenti, J. 2005, *ApJ*, 622, 1102
- François, P., Pasquini, L., Biazzo, K., Bonifacio, P., & Palsa, R. 2013, *A&A*, 552, AA136
- Ghezzi, L., Cunha, K., Smith, V. V., & de la Reza, R. 2010, *ApJ*, 724, 154
- Gonzalez, G. 1998, *A&A*, 334, 221
- Gonzalez, G. 2008, *MNRAS*, 386, 928
- Gonzalez, G. 2014, *MNRAS*, 441, 1201
- Gonzalez, G. 2015, *MNRAS*, 446, 1020
- Gray, R. O., Graham, P. W., & Hoyt, S. R. 2001, *AJ*, 121, 2159
- Hunten, D. M., Wells, W. K., Brown, R. A., Schneider, N. M., & Hilliard, R. L. 1991, *PASP*, 103, 1187
- Israelian, G., Santos, N. C., Mayor, M., & Rebolo, R. 2004, *A&A*, 414, 601
- Israelian, G., Delgado Mena, E., Santos, N. C., et al. 2009, *Nature*, 462, 189
- Lambert, D. L., & Reddy, B. E. 2004, *MNRAS*, 349, 757
- Li, T. D., Bi, S. L., Yang, W. M., et al. 2014, *ApJ*, 781, 62
- López-Valdivia, R., Bertone, E., Chávez, M., et al. 2014, *MNRAS*, 444, 2251
- Kupka, F., Piskunov, N., Ryabchikova, T. A., Stempels, H. C., & Weiss, W. W. 1999, *A&AS*, 138, 119
- Kurucz, R. L., Furenlid, I., Brault, J., & Testerman, L. 1984, *National Solar Observatory Atlas Sunspot*, New Mexico: National Solar Observatory, 1984,
- Li, T. D., Bi, S. L., Chen, Y. Q., et al. 2012, *ApJ*, 746, 143
- Luck, R. E., & Heiter, U. 2006, *AJ*, 131, 3069
- Mishenina, T. V., Soubiran, C., Kovtyukh, V. V., Katsova, M. M., & Livshits, M. A. 2012, *A&A*, 547, AA106
- Monaco, L., Villanova, S., Bonifacio, P., et al. 2012, *A&A*, 539, AA157
- Montalbán, J., & Schatzman, E. 2000, *A&A*, 354, 943
- Önehag, A., Gustafsson, B., & Korn, A. 2014, *A&A*, 562, AA102
- Pace, G., Castro, M., Meléndez, J., Théado, S., & do Nascimento, J.-D., Jr. 2012, *A&A*, 541, AA150
- Pinsonneault, M. H., Deliyannis, C. P., & Demarque, P. 1992, *ApJS*, 78, 179
- Ramírez, I., Fish, J. R., Lambert, D. L., & Allende Prieto, C. 2012, *ApJ*, 756, 46
- Ryan, S. G. 2000, *MNRAS*, 316, L35
- Santos, N. C., Israelian, G., & Mayor, M. 2001, *A&A*, 373, 1019
- Schaeuble, M., & King, J. R. 2012, *PASP*, 124, 164
- Schatzman, E., & Baglin, A. 1991, *A&A*, 249, 125
- Scholz, A., Coffey, J., Brandeker, A., & Jayawardhana, R. 2007, *ApJ*, 662, 1254
- Snedden, C.A. 1973, Ph.D. Thesis, University of Texas, Austin
- Swenson, F. J., & Faulkner, J. 1992, *ApJ*, 395, 654
- Takeda, Y., Ohkubo, M., Sato, B., Kambe, E., & Sadakane, K. 2005, *PASJ*, 57, 27
- Takeda, Y., Honda, S., Kawanomoto, S., Ando, H., & Sakurai, T. 2010, *A&A*, 515, AA93
- Takeda, Y., Honda, S., Ohnishi, T., et al. 2013, *PASJ*, 65, 53
- Théado, S., & Vauclair, S. 2012, *ApJ*, 744, 123
- Xing, L. F. 2010, *ApJ*, 723, 1542
- Xing, L.-F., Zhao, S.-Y., & Zhang, X.-D. 2012, *NewA*, 17, 537
- Xing, L.-F., & Xing, Q.-F. 2012, *A&A*, 537, AA91